Available online at www.sciencedirect.com

jmr&t Journal of Materials Research and Technology

journal homepage: www.elsevier.com/locate/jmrt

Original Article

Performance of Al_2O_3/TiC mixed ceramic inserts coated with TiAlSiN, WC/C and DLC thin solid films during hard turning of AISI 52100 steel

Ch Sateesh Kumar [a,*], *Saroj Kumar Patel* [b], *Filipe Fernandes* [c,d]

[a] *Department of Mechanical & Industrial Engineering Technology, University of Johannesburg, South Africa*
[b] *Department of Mechanical Engineering, National Institute of Technology, Rourkela, Odisha-769008, India*
[c] *University of Coimbra, CEMMPRE - Centre for Mechanical Engineering Materials and Processes, Department of Mechanical Engineering, Rua Luís Reis Santos, 3030-788 Coimbra, Portugal*
[d] *ISEP - School of Engineering, Polytechnic of Porto, Rua Dr. António Bernardino de Almeida 431, 4200-072 Porto, Portugal*

ARTICLE INFO

Article history:
Received 19 April 2022
Accepted 17 June 2022
Available online 23 June 2022

Keywords:
Hard machining
Mixed ceramic cutting tools
DLC coating
WC/C coating
TiAlSiN coating

ABSTRACT

The present work evaluates the turning performance of alumina (Al_2O_3) and titanium carbide (TiC) based mixed ceramic cutting inserts with TiAlSiN, WC/C and DLC thin-film depositions during machining of AISI 52100 steel hardened to 55 ± 2 HRC hardness. Based on the generated machining forces, coefficient of friction, geometrical characteristics of the chips, and tool wear, a comparative analysis of the performance of uncoated and coated cutting tools was carried out. The machining outcomes were interpreted in relation to the adhesion strength of coating with the substrate, surface roughness and hardness of the top surface of the coatings. It was observed that the reduction of friction and machining forces accounted to lower localized strain along the shear plane leading to lower deformation of the chips. The TiAlSiN coating exhibited superior wear-resistance at the highest cutting speed when compared to DLC and WC/C coatings owing to its higher hardness and higher coating/substrate adhesion strength. However, the DLC and WC/C coatings, although softer, accounted to significant reduction of machining forces due to their self-lubricating properties.

1. Introduction

It is known that the metal cutting or machining plays a significant role in the development of engineered parts and components. The continuous evolution of materials and increasing demand for machining the materials without processing necessitates researchers and engineers to continue research and development in the machining technology to investigate and develop new materials, coatings, and treatments for cutting tools. Also, the development of novel lubrication techniques, systems, and lubricants is being

* Corresponding author.
E-mail address: chigulla51@gmail.com (C.S. Kumar).
https://doi.org/10.1016/j.jmrt.2022.06.092

considered as a way to minimize energy and resource consumption [1–3]. Hardened steels that are used for production of gears, camshafts, bearings and other mechanical transmission parts are considered difficult-to-machine materials due to their high hardness. Thus, investigating the machinability of hardened steel with various types of cutting tools, has become an attractive topic for the researchers [4–6]. Further, the literature shows that the cutting tool material and its geometry have grave significance due the high tool wear, machining forces and cutting temperatures associated with the machining process of hardened steel [7,8]. In this regard, two important past studies we would like to highlight. Sales et al. [9] during the performance study of Al_2O_3/TiC and PCBN-H cutting tools revealed that the economical Al_2O_3/TiC ceramic composite tool didn't surpass the machining performance of superior PCBN-H tool but the performance was acceptable if the high cost of the PCBN-H tool is considered. Similarly, Sobiyi et al. [10] compared the performance of CBN and alumina (Al_2O_3) based ceramic composite cutting tools during machining of martensitic stainless steel and revealed similar results for mixed ceramic cutting tools. Thus, it can be concluded that the mixed ceramic tools can act as a replacement to the costly PCBN or CBN cutting tools due to their comparable and acceptable performance, and also, due to the economic aspects if the cost of the tooling is considered.

The shortcomings of the mixed ceramic cutting tools can be covered up to some extent by deposition of thin-films that can improve the wear-resistance, thermal and chemical stability, and mechanical deterioration that would subsequently add to the durability of the cutting tools [11–13]. In a very important investigation, the present authors [14] reported that the TiAlSiN nanocomposite coating significantly extended the machining performance of the Al_2O_3/TiCN ceramic composite cutting tools. Various researchers have reported similar studies for mixed ceramic or ceramic composite cutting tools [9,15,16]. Low-friction and self-lubricating coatings, in addition to hard coatings, have improved the machining performance of cutting tools [17–20]. A past study reports that the deposition of DLC and WC/C low friction coatings over the Al_2O_3/TiCN based composite ceramic cutting tools resulted in a considerable improvement in the machining performance of AISI 52100 steel during hard turning [21]. However, low friction coating application during hard machining is still limited. Moreover, investigations pertaining to chip morphology during hard machining using coated mixed ceramic cutting tools is also scarce.

According to the literature, the majority of the research done so far on coated mixed ceramic cutting tools has been focused on evaluating tool wear and other tribological factors throughout the machining process. However, chip morphology studies have been mostly neglected. Further, the suitable use of hard and soft coatings to extend the service life of the mixed ceramic cutting tools has been discussed separately and thus, a comparative analysis is lacking in the literature. Thus, a comprehensive exploration of the benefits and shortcomings of both the type of coatings during hard machining application is necessary. As a result, the current study compares the performance of TiAlSiN, DLC, and WC/C coated Al_2O_3/TiC mixed ceramic cutting tools when hard turning AISI 52100 steel at various cutting speeds. Uncoated Al_2O_3/TiC mixed ceramic tools were also tested for comparison purposes.

2. Experimental methodology

2.1. Coatings deposition and characterization

Sputtering was used to deposit all of the coatings on the Al_2O_3/TiC mixed ceramic tools with the SNGA120408 designation. Pure graphite targets were utilised to deposit the DLC coating, while tungsten targets were employed to deposit the WC/C coating in addition to graphite targets. The DLC coating was made in a hydrogenated type DLC-a-C:H - under a reactive environment of CH_4. WC/C, on the other hand, is a type of DLC coating that incorporates WC doping to create an Me-a-C:H structure. WC/C is a multi-layered coating with alternate WC and C layers, whereas DLC is a mono-layered coating. The coatings produced are ~2 μm thick. The TiAlSiN coating was produced from 99.95% purity targets of TiSi and TiAl with target power of 5 kW in a nitrogen reactive atmosphere using direct current reactive magnetron sputtering process (DCRMS). The coating chamber was maintained at a pressure of 570 mPa whereas N_2 was introduced at 270 mPa and Ar at 350 mPa pressures respectively. A bias voltage of −450 V with 20 A current was used. The temperature inside the chamber measured at 400–500 °C during the coating process. At this high temperature, the nanocomposite structure is well known to be formed. Indeed, for such deposition temperatures spinodal composition occurs and segregation of Si–N phase to the grain boundaries happens, producing a nanocomposite structure [22]. The TiAlSiN coating was ~3 μm thick. Before the deposition of the coatings the Al_2O_3/TiC mixed ceramic substrates were heated and ion etched by using a mixture of argon and krypton gas to enhance the coating/substrate adhesion strength and avoid any possible surface contaminations.

After the deposition process, the surface roughness was analysed using Taylor Hobson surface roughness tester. The surface roughness measurements were made ten times at different locations and an average was determined from the values. The hardness of the coatings was determined using a Nanoindentation tester equipped with a sharp Berkovich indenter. Ten different readings were made with a load of 10 mN, loading rate of 20 mN/min, and dwell time of 5 s. Later the readings were averaged on each type of coated tool to determine the final value. The indentation depth was <10% of the films thickness, to eliminate the substrate contribution. The scratch testing using Ducom's scratch tester was performed on the coated tools using a Rockwell C indenter of radius of 0.2 mm, increasing the force linearly from 5 N to 80 N. The readings were taken at ten different locations to determine the average coating/substrate adhesion strength corresponding to each coating and substrate pair. The tests were carried out under a scratch speed of 0.2 mm/s and a loading rate of 20 N/mm. Adhesion critical loads were determined by optical microscope analysis. The scratch testing using Ducom's scratch tester was performed on the coated

tools at ten different locations to determine the average coating/substrate adhesion strength corresponding to each coating and substrate pair.

2.2. Turning tests

Fig. 1 shows the experimental setup for the turning tests. The tests were performed with a cutting tool having designation SNGA120408 and made of Al_2O_3/TiC ceramic material. Further, the tool holder used for the tests had a designation of PSBNR202020K12. AISI 52100 steel hardened to 55 ± 2 HRC was used as the workpiece material. Uncoated Al_2O_3/TiC ceramic cutting tool and coated tools with of DLC, WC/C, and TiAlSiN coatings were subjected to turning tests under dry cutting environment with a depth of cut of 0.5 mm and feed rate of 0.16 mm/rev. During experiments, the cutting speed was varied from 100 m/min to 250 m/min with an interval of 50 m/min. Each experimental test was conducted thrice to ensure the reproducibility of the results.

2.3. Measurements

The machining forces were measured using Kistler made Piezoelectric dynamometer which was equipped with a charge amplifier for recording the force values. After the turning tests, the chips were collected and geometrical measurements were made on the SEM micrographs of the back and free surface of the chips. Fig. 2 shows the various geometrical parameters measured on the SEM micrographs of the chips formed while machining with the cutting tools. The chip thickness was measured using digital Vernier Callipers. The chip-thickness, chip-width, major teeth height, minor teeth height and teeth bend angle were measured on thirty different locations and an average was considered as the final reading. This extensive process was adopted to avoid machining and measurement errors. Scanning electron microscopy was also used to investigate wear on the flank and rake surfaces of uncoated and coated cutting tools.

2.4. Finite element simulations

The observations on the measured chip–geometrical parameters require further investigation on localized stress and strain generated in the chips during formation of serrated teeth. Thus, a 2D finite element model has been developed using Deform 2D (Version 10.2) software package to investigate the above observations more precisely. The model adopts the flow stress behaviour of the AISI 52100 steel from the hardness-based flow stress model proposed by Umbrello et al. [3] which may be expressed as:

$$\sigma(\varepsilon, \dot{\varepsilon}, t, R) = X(t)(I\varepsilon^n + Y + Z\varepsilon)(1 + (\ln(\varepsilon) - H)) \quad (1)$$

where

$$X(t) = e^{(at^5+bt^4+ct^3+dt^2+et+f)} \quad (2)$$

$$Y = 27.4R - 1700.2 \quad (3)$$

$$Z = 4.48R - 279.9 \quad (4)$$

where ε is the effective strain, $\dot{\varepsilon}$ is the effective strain rate ($1.0s^{-1}$), R (55 HRC) is the hardness of the material, and t is the temperature in degree Celsius. The other material constants of the model have been listed in Table 1. The adopted flow stress model considers the effect of hardness on the strain hardening property of the workpiece material.

The mechanical and thermal properties of the AISI 52100 steel workpiece material, Al_2O_3/TiC cutting tool material and the coatings (TiAlSiN, DLC and WC/C) have been adopted from the literature [12,21,23–28]. The thermal expansion and emissivity of the coatings have been assumed equal to the substrate material. All the finite element simulations were carried out at a cutting speed of 250 m/min with 0.16 mm/rev feed rate and 0.5 mm depth of cut. The finite element study is basically focused on the localized effective strain during formation of the serrated teeth and the stress generation in the localized region just before the separation of serrated layer

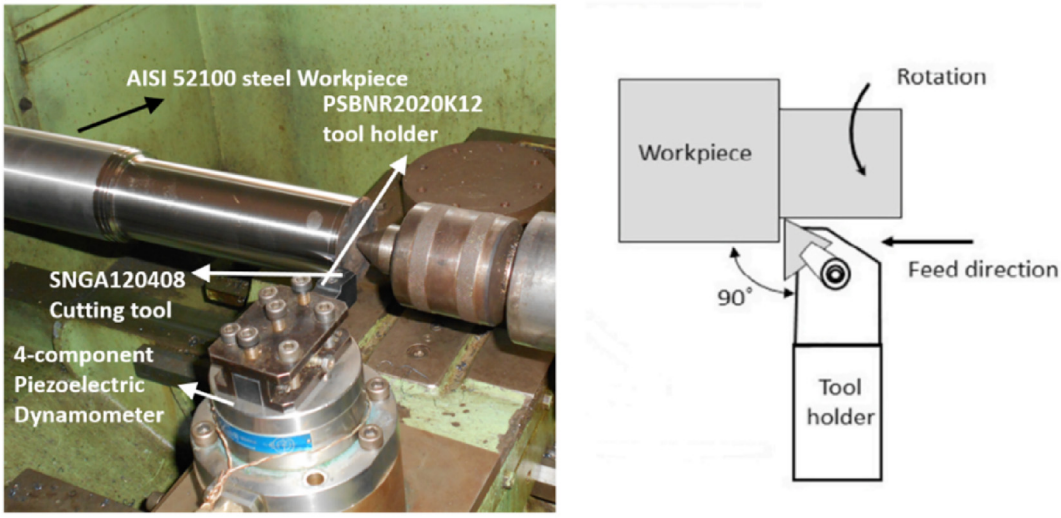

Fig. 1 – Experimental setup for turning with Kistler Piezoelectric Dynamometer attachment for force measurement.

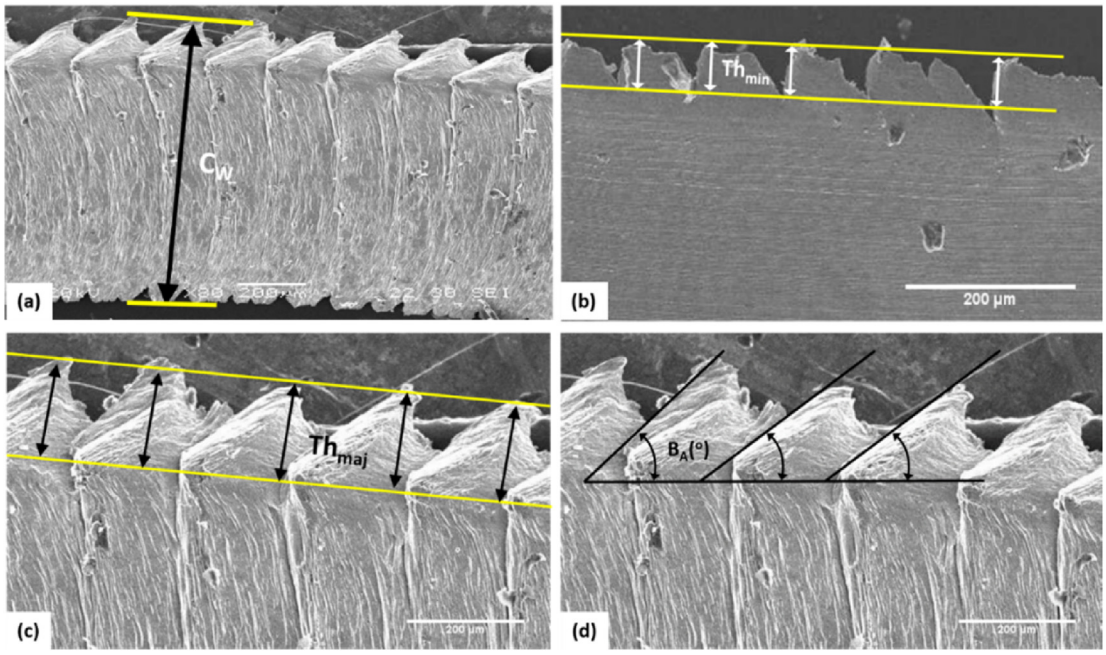

Fig. 2 – SEM micrographic images of the chips showing measurement of (a) chip width, C_W, (b) minor teeth height, Th_{min}, (c) major teeth height, Th_{maj}, and (d) teeth bend angle, B_A(°).

and thus, the tool is considered rigid during the simulations. Further, Coulomb's friction criterion has been considered for defining the interaction between the tool and the workpiece. Brozzo's damage criterion [2] has been adopted to define the failure mechanism in the workpiece material which also facilitates formation of serrated teeth during numerical simulations.

3. Results and discussion

3.1. *Coating characterization*

The deposited coatings have been characterized based on the average coating-surface roughness (R_a), coating/substrate adhesion strength, and surface hardness obtained from nanoindentation tests. The coating/substrate adhesion strength significantly impacts flaking and coating delamination during the machining process and thus, it becomes an important parameter to be investigated. The scratch tests revealed that the low-friction DLC and WC/C coatings on the Al_2O_3/TiC ceramic substrate exhibited first critical load Lc1 of 38 N and 56 N for first coating cracking indicating low coating/substrate adhesion strength. On the contrary, the TiAlSiN coating exhibited excellent coating/substrate adhesion strength with a Lc1 critical load of 75 N. TiAlSiN and WC/C coatings only displayed Lc1 (first coating cracking) type adhesion failure. However, DLC coating displayed all the three types of failure modes namely; Lc1, Lc2 (first coating chipping) and Lc3 (more than 50% of the coating failure).

Further, it was observed that the measured hardness using the nanoindentation tests of the low-friction DLC (22.27 ± 1.23 GPa) and WC/C (13.95 ± 0.83 GPa) coatings was even lower than that of the ceramic substrate (27.72 ± 1.51 GPa). Thus, WC/C and DLC coatings can be termed as soft-coatings attributing to their hardness which is lower than that of the Al_2O_3/TiC substrate. From the literature it is evident that the doping can reduce hardness of DLC thin-films whereas it is beneficial in increasing the adhesion to the substrate [29,30] and thus, there is a reduction of hardness and increase of adhesion strength for the WC/C coating. However, the TiAlSiN coating due its nanocomposite structure exhibited a high value of hardness of 38.83 ± 1.47 GPa, that satisfies the condition of hard coating. Further, it has been observed that the coated surfaces exhibited significantly low values of average surface roughness R_A (0.16 ± 0.03 µm for WC/C, 0.13 ± 0.02 µm for DLC and 0.17 ± 0.02 µm for TiAlSiN coating) when compared to the uncoated ceramic tool's surface roughness (0.32 ± 0.05 µm).

Table 1 – AISI 52100 steel hardness-based flow stress model material constants.

Material constant	Value	Material constant	Value
a	3.8121 x E−15	f	0.02443
b	−3.2927 x E−12	I	1092 MPa
c	−6.9118 x E−9	n	0.083
d	5.4993 x E−6	m	0.1259
e	−1.2419 x E−3	H	0.0567

3.2. *Effect on machining forces*

The variation of machining forces, namely feed force F_X, cutting force F_Y, and thrust force F_Z, with cutting speed are depicted in Fig. 3. Machining using coated tools resulted in machining force reductions at all cutting speeds, with a maximum decrease of 45 percent in feed force, 32 percent in cutting force, and 41 percent in thrust force. The largest

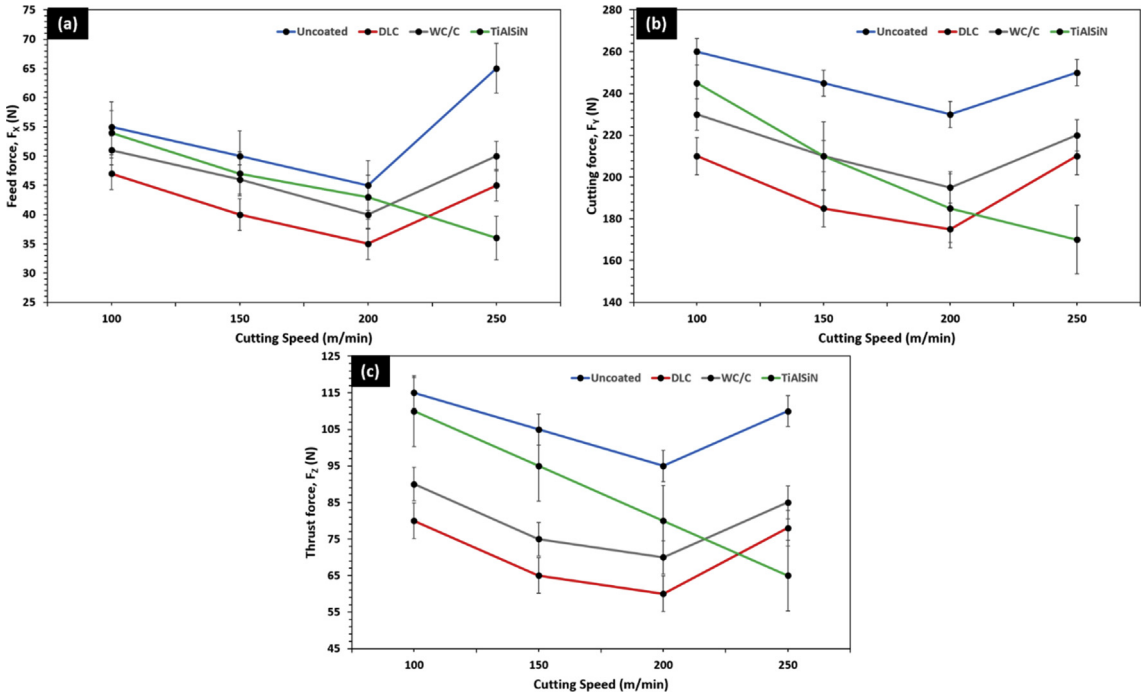

Fig. 3 – Variation of (a) feed force, F_X, (b) cutting force, F_Y and (c) thrust force, F_Z for uncoated and coated Al_2O_3/TiC mixed ceramic cutting tools as a function of cutting speed.

reductions corresponded to the TiAlSiN coated tool at a cutting speed of 250 m/min, which necessitates more examination into tool wear, which will be detailed in Section 3.5. It was also discovered that when the cutting speed increased, the machining forces decreased. However, an unusual behaviour was seen for uncoated, DLC coated, and WC/C coated tools at the greatest cutting speed of 250 m/min. It was observed that the machining forces associated with these tools decreased up to 200 m/min cutting speed, however at 250 m/min cutting speed, all tools except the tool coated with TiAlSiN resulted in increase of machining forces. This behaviour can be attributed to the combination effect of high cutting temperatures prevailing at 250 m/min, low hardness and oxidation resistance of the low friction films. Further, coating delamination and sub-standard coating/substrate adhesion of the DLC and WC/C coatings may have also led to this increase in machining forces. The TiAlSiN coated tool, on the other hand, resulted in a further reduction in machining forces at 250 m/min, which is basically due to the higher coating/substrate adhesion strength, high oxidation and wear-resistance offered by the nanocomposite coating.

Furthermore, when compared to the uncoated tool, the percentage reduction in machining forces for DLC and WC/C coated tools decreased with increasing cutting speed up to 200 m/min, and at 250 m/min cutting speed, the percentage reduction increased, indicating severe tool wear for the uncoated cutting tool. Moreover, the percentage reduction in machining forces for DLC and WC/C coated tools demonstrated an inclination of their performance toward uncoated tools as cutting speed increased. On the other hand, for the TiAlSiN coated tool, the inverse phenomenon can be observed, i.e., the percentage reduction in machining forces increased with increasing cutting speed up to 250 m/min, indicating higher thermal stability and wear resistance for the TiAlSiN coating. Consequently, the better coating/substrate adhesion strength, thermal stability and oxidation resistance of the coating resulted in a superior performance of the inserts under harsh machining conditions. However, this phenomenon requires detailed wear study which will be covered in Section 3.5.

3.3. *Effect on apparent coefficient of friction (μ_{ap})*

During a metal cutting operation, friction at the cutting zone plays an important role in determining the performance of cutting tools. Further, during machining of hardened steel like 52,100 steels, friction becomes more significant parameter due to the associated high temperature and machining forces. In this regard, the coefficient of friction during the cutting process, termed as 'apparent coefficient of friction (μ_{ap})' has been evaluated by converting a three-dimensional force system into a two-dimensional system for simplicity and then the μ_{ap} has been determined using the equation below.

$$\mu_{ap} = \frac{F_Y + F_{XZ} tan\alpha}{F_Y - F_{XZ} tan\alpha} \quad (5)$$

where, F_Y is the cutting force and F_{XZ} is the equivalent thrust force that can be further expressed as:

$$F_{XZ} = \sqrt{F_X{}^2 + F_Z{}^2} \quad (6)$$

Wwhere F_X is the feed force and F_Z is the thrust force.

Fig. 4 shows the assessed values of μ_{ap} for both coated and uncoated cutting tools plotted versus cutting speed. Deposition of low-friction coatings on the ceramic cutting tool has resulted in a significant reduction in friction at the cutting zone. This is due to their low-friction and self-lubricating characteristics (DLC and WC/C coatings). On the contrary,

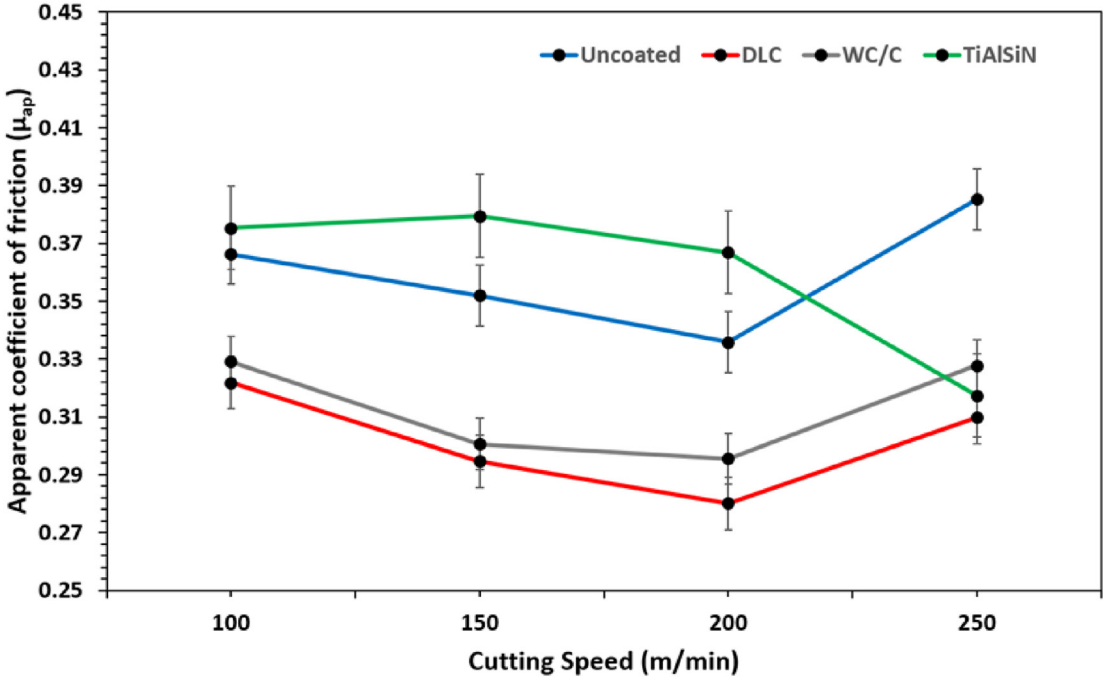

Fig. 4 – Fluctuation of apparent coefficient of friction (μ_{ap}) for uncoated and coated Al_2O_3/TiC mixed ceramic cutting tools as a function of cutting speed.

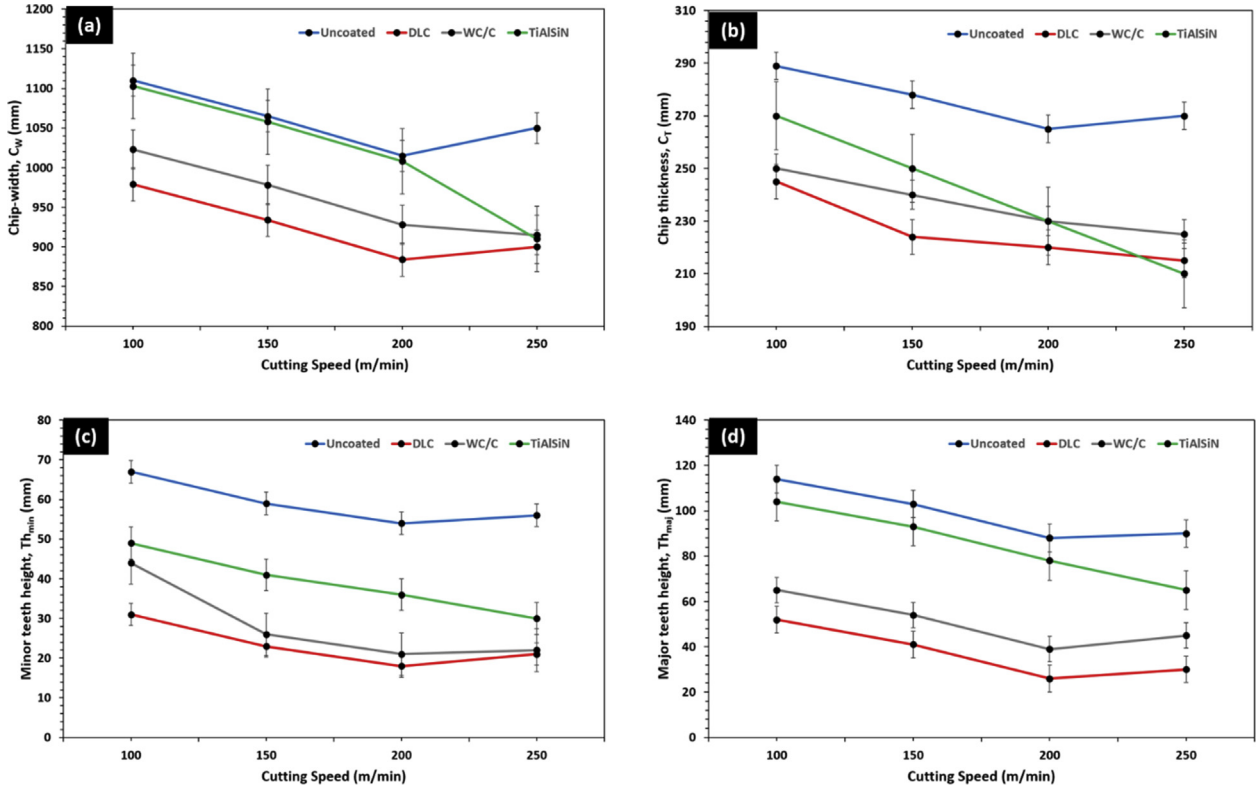

Fig. 5 – Variation of (a) chip width, C_W, (b) chip thickness, C_T (c) minor teeth height, Th_{min}, and (d) major teeth height, Th_{maj} for uncoated and coated Al_2O_3/TiC mixed ceramic cutting tools as a function of cutting speed.

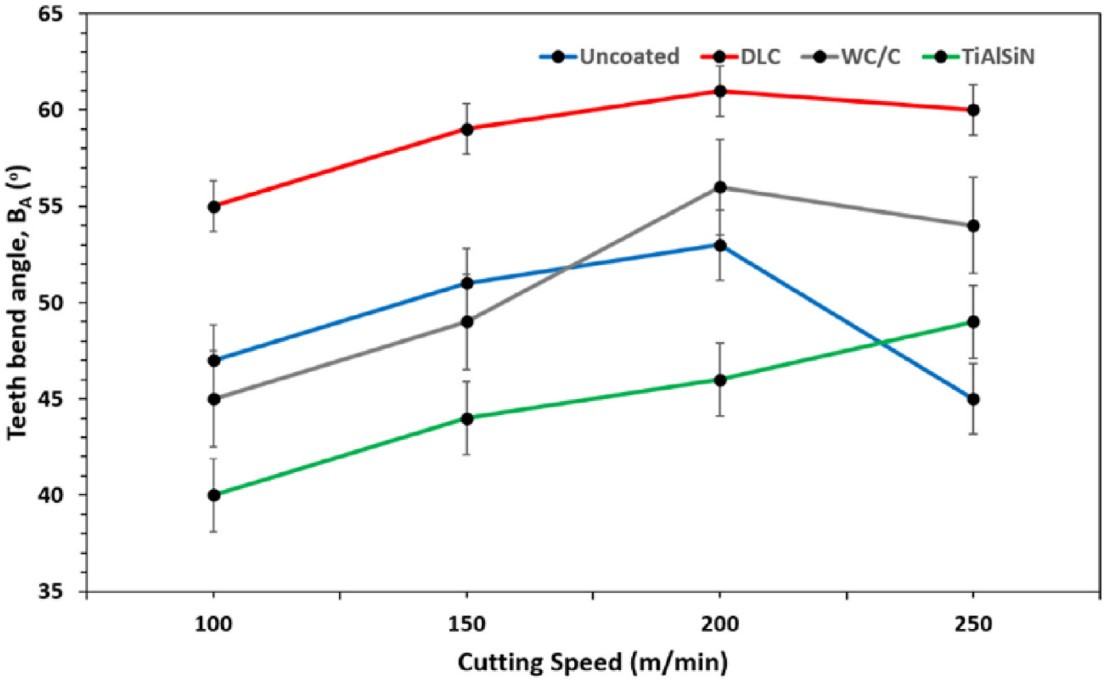

Fig. 6 – Fluctuation of teeth bend angle, B_A(°) for uncoated and coated Al_2O_3/TiC mixed ceramic cutting tools as a function of cutting speed.

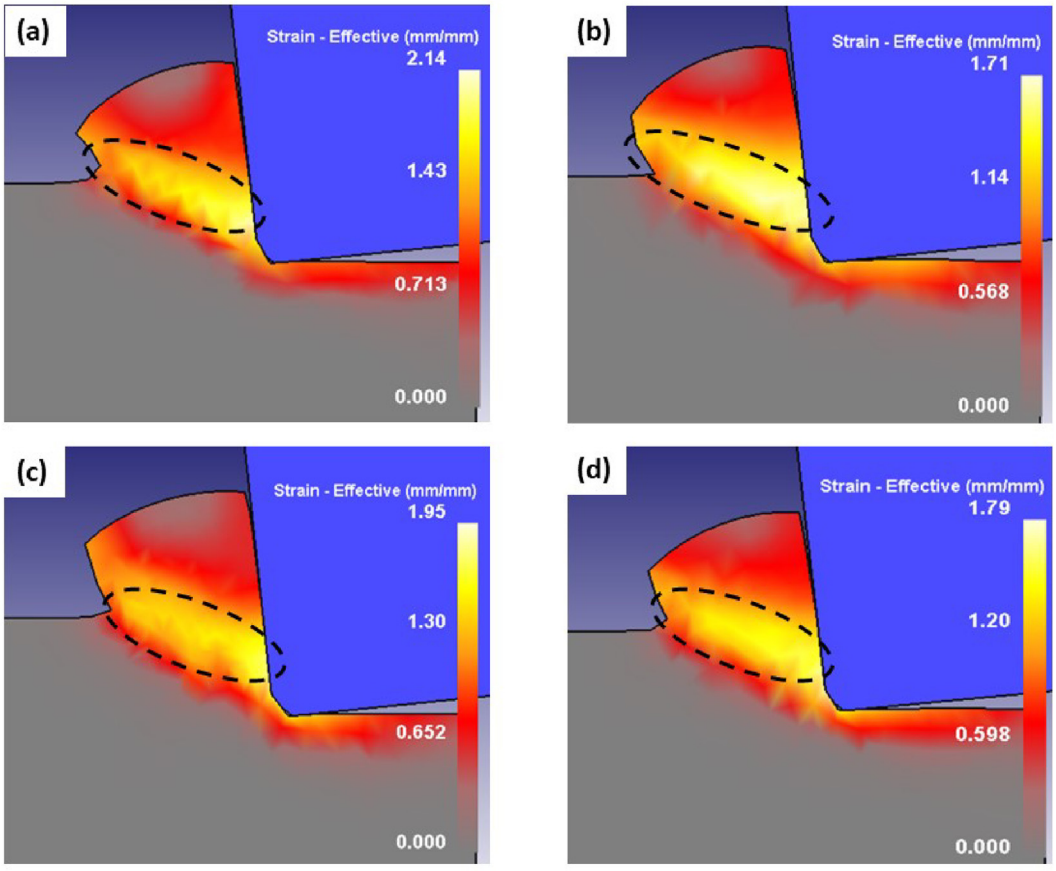

Fig. 7 – Localized strain along the shear plane for (a) uncoated, (b) DLC coated, (c) WC/C coated and (d) TiAlSiN coated Al_2O_3/TiC cutting tools.

TiAlSiN coating displayed slight high μ_{ap} than the other coatings up 200 m/min. However, at the highest cutting speed of 250 m/min, the μ_{ap} of TiAlSiN coating suddenly drop accounting to lower friction coefficient as compared to the uncoated cutting tool and to aq similar μ_{ap} as the other coatings. The TiAlSiN coating's superior coating/substrate adhesive strength, as well as its considerably higher hardness, have allowed it to withstand the tremendous thermal stresses induced at the highest cutting speed of 250 m/min. In fact, at 250 m/min cutting speed, the TiAlSiN coated tool had a lower coefficient of friction than the WC/C coated tool, but the difference was insignificant. Further, it was observed that the DLC coated cutting tool corresponded to lower coefficient of friction under all conditions owing to the superior self-lubricating properties of DLC coating due to formation of graphite during the machining process [23,31].

3.4. *Effect on chip morphology*

3.4.1. *Effect on chip geometry*

Effect of thin-film depositions on the chip formation has been elaborated and discussed by various researchers [32–35]. However, the influence of low-friction or self-lubricating coatings has not been specifically investigated and compared with performance of hard coatings. Thus, the current study investigates the effect of coating depositions on chip formation during machining of hardened AISI 52100 alloy steel. Fig. 5 shows how chip width (C_w), chip thickness (C_T), major teeth height (Th_{maj}), and minor teeth height (Th_{min}) vary as cutting speed increases. For uncoated, DLC, and WC/C coated tools, the C_w, C_T, Th_{maj}, and Th_{min} dropped as the cutting speed increased up to 200 m/min. However, an increase in C_w, C_T, Th_{maj}, and Th_{min} can be seen at the cutting speed of 250 m/min. C_w, C_T, Th_{maj}, and Th_{min} decreased with increasing cutting speed for TiAlSiN coated tools until the maximal cutting speed of 250 m/min. This peculiar behaviour can be attributed to the variation of machining forces with the cutting speed. Also, a close relation between the coefficient of friction and measured chip-dimensions can be developed. The chip–geometry parameters are found to be linearly related to the coefficient of friction, with lower coefficients of friction leading to reduced chip–geometry parameters and vice versa. A lower value of friction coefficient accounted to lower deformation in the generated chips eventually leading to lower values of C_w, C_T, Th_{maj}, and Th_{min}.

Comparatively, the teeth bend angle (B_A) increases with the increase of cutting speed (see Fig. 6). The variation B_A can be related inversely to the coefficient of friction. It was observed that the lower coefficient of friction leads to lesser bending stresses on generated serrated teeth leading to higher chip

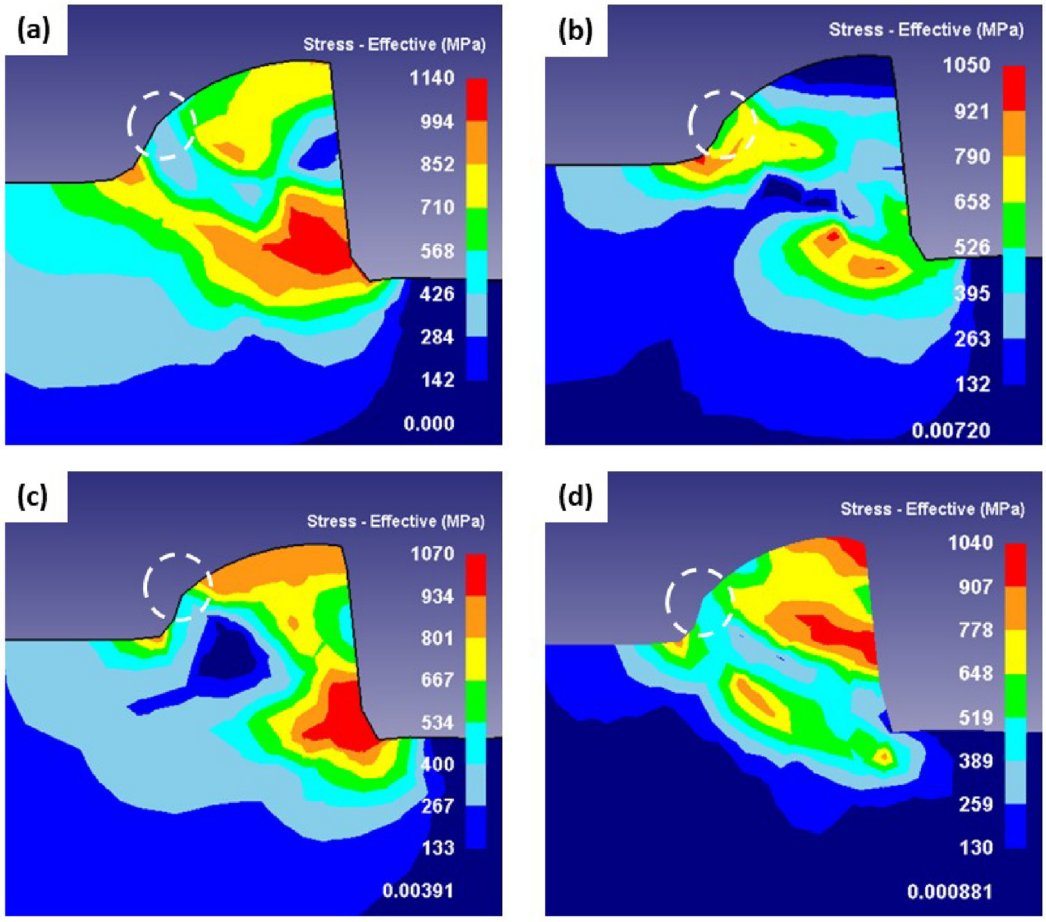

Fig. 8 – Localized stress at the tip of the serrated teeth for (a) uncoated, (b) DLC coated, (c) WC/C coated and (d) TiAlSiN coated Al_2O_3/TiC cutting tools.

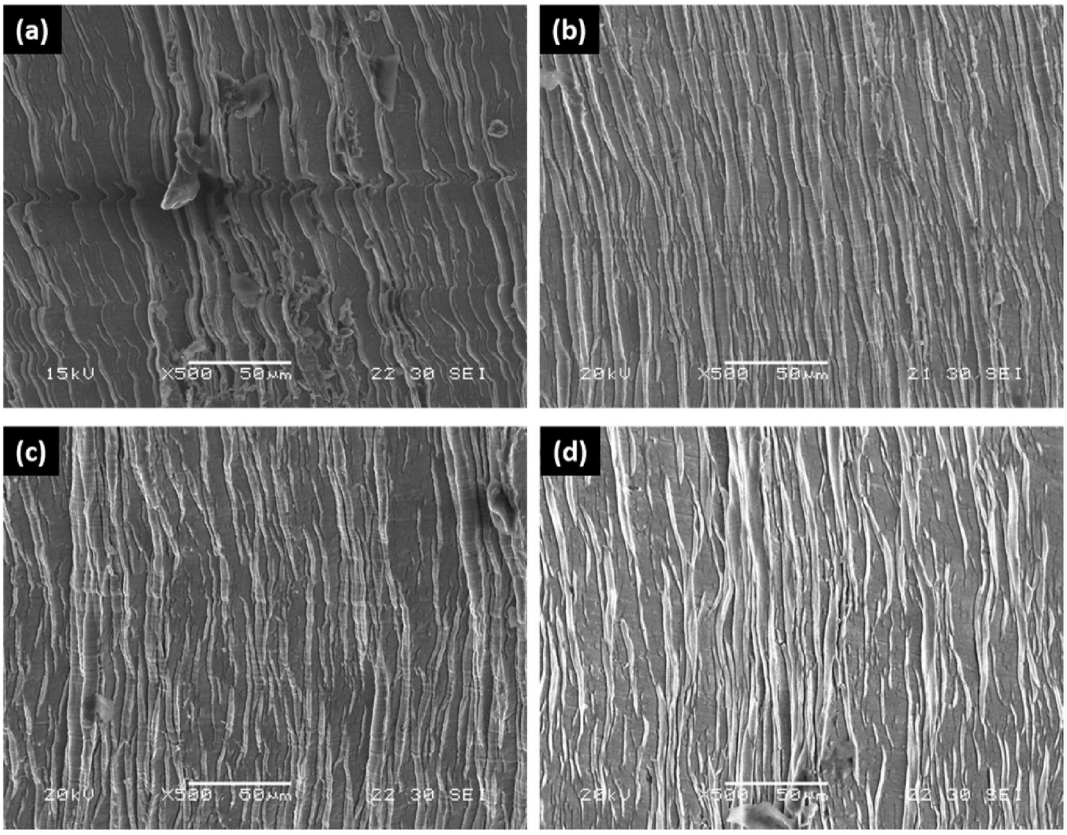

Fig. 9 – SEM micrographic images of the free surface of the chips formed while machining at 250 m/min cutting speed with (a) uncoated, (b) DLC coated, (c) WC/C coated and (d) TiAlSiN coated Al_2O_3/TiC cutting tools.

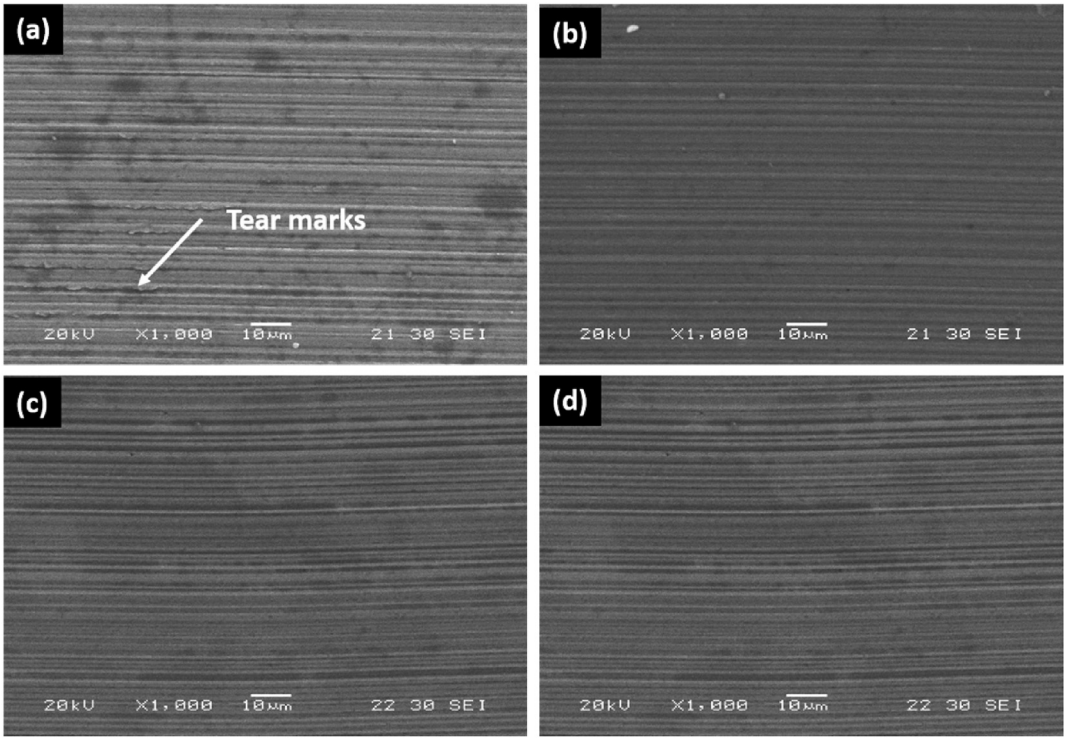

Fig. 10 – SEM micrographic images of the back (machined surface) surface of the chips formed while machining at 250 m/min cutting speed with (a) uncoated, (b) DLC coated, (c) WC/C coated and (d) TiAlSiN coated Al_2O_3/TiC cutting tools.

bend angles. In order to precisely understand this phenomenon, localized stress at the tip of the serrated chip has to be studied which has been carried out using finite element analysis in Section 3.4.2.

3.4.2. *Localized stress and strain in chips*

Fig. 7 shows the localized strain along the shear plane in the generated chips while machining with uncoated and coated cutting tools. It can be seen that the localized strain is

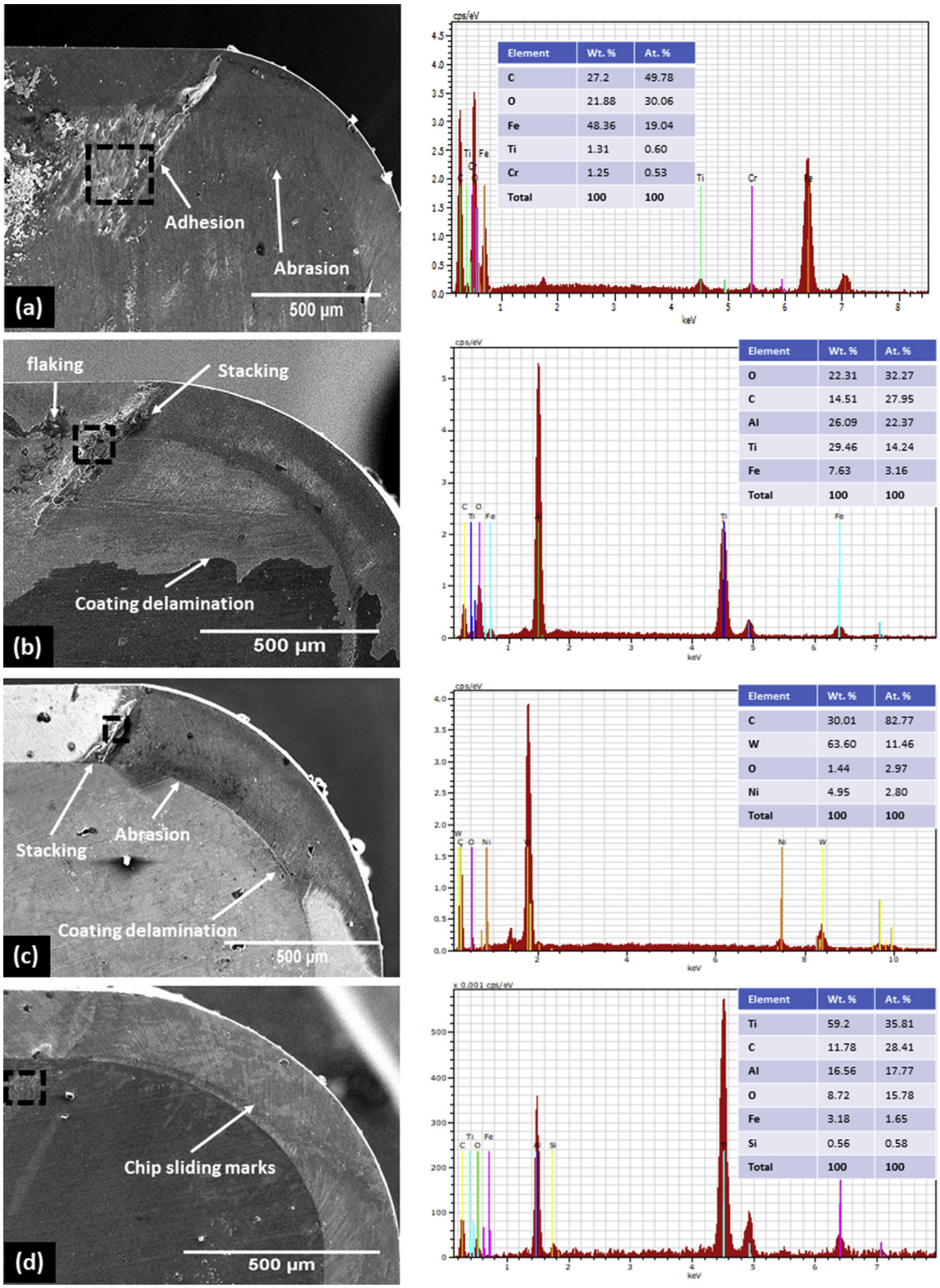

Fig. 11 – SEM micrographic images of the rake surface while machining at 250 m/min cutting speed with (a) uncoated, (b) DLC coated, (c) WC/C coated and (d) TiAlSiN coated Al_2O_3/TiC cutting tools.

dependent on the coefficient of friction with lower frictional coefficient corresponding to lower effective localized strain and vice versa. The higher localized strain accounted to higher values of C_w, C_T, Th_{maj}, and Th_{min} and vice versa. Further, when the stress in the marked region in Fig. 8 is studied, it can be seen that the higher coefficient of friction led to lower values of localized stress on the tip of the initiated serrated teeth. Thus, lower localized stress at higher coefficient of friction has resulted in lower chip bend angles at higher coefficient of friction values.

3.4.3. *SEM morphology of chips*

The free and back surfaces of chips generated when machining with uncoated and coated cutting tools are shown in Figs. 9 and 10 respectively. On the free surface of coated cutting tools, a unique observation has been made. When machining with coated cutting tools, the free surface showed a more uniform distribution of serration layers than the chips corresponding to the uncoated tool. In addition, as compared to the uncoated cutting tool, the layered distribution suggested that machining with coated tools accounted to lower strain on the serrated layers, which might be attributed to lower associated machining forces and friction. The machined surface (back surface), on the other hand, has a direct relationship with the coefficient of friction, with lower friction values corresponding to a smoother machined surface.

3.5. *Effect on tool wear*

3.5.1. *Crater wear*

Fig. 11 shows the rake surface for the cutting tools at 250 m/min cutting speed. The wear on the rake face of the uncoated Al_2O_3/TiC cutting tool is characterized by adhesion and abrasion whereas for DLC and WC/C coated tools the wear is characterized by flaking, coating delamination and stacking in addition to adhesion and abrasion. On the contrary, for the TiAlSiN coated tool, the wear was basically in form of adhesion with negligible abrasion. A substantial adhesion region has been developed for the uncoated ceramic cutting tool whereas the coated tools exhibited excellent anti-adhesive properties on the rake face with minimal material adhesion which is apparent from the EDS analysis of the marked regions. Although the DLC coating accounted to very low values of coefficient of friction, significant coating delamination and flaking can be seen on the DLC coated tool with has occurred because of the lower coating/substrate adhesion strength. However, the coating delamination and formation of graphite at high temperatures [23,31], led to the accumulation of lubricant (in this case graphite) at the chip–tool interface leading to formation of low-friction zone when the chips slide over the rake face satisfying the self-lubricating properties of the DLC coating. On the contrary, when compared to the DLC coated cutting tool, delamination was not as severe for the WC/C coated tool.

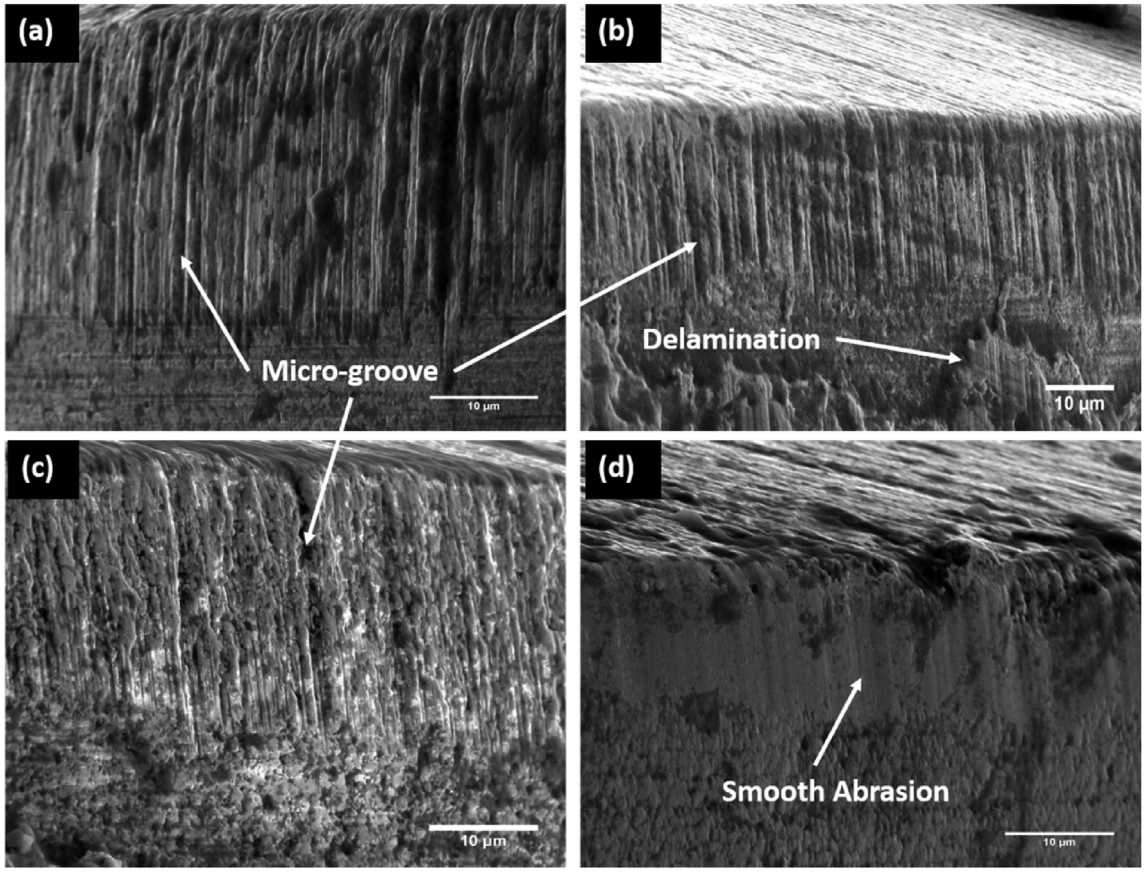

Fig. 12 – SEM micrographic images of the flank surface while machining at 250 m/min cutting speed with (a) uncoated, (b) DLC coated, (c) WC/C coated and (d) TiAlSiN coated Al_2O_3/TiC cutting tools.

On the rake surface of both DLC and WC/C coated mixed ceramic cutting tools, however, material stacking owing to coating delamination and chip movement is observed. Furthermore, when compared to the uncoated tool, abrasion on the rake surface for the DLC and WC/C coated tools was smoother. Even at the greatest cutting speed of 250 m/min, the TiAlSiN coated tool showed no signs of wear and or delamination. The TiAlSiN coated tool's enhanced performance can be due to the TiAlSiN coating's higher coating/substrate adhesion strength, hardness, thermal stability and oxidation resistance.

3.5.2. *Flank wear*

Further, when the flank surface of the cutting tools was analysed, similar trend can be observed for the coated cutting tools. At a cutting speed of 250 m/min, wear behaviour on the flank surface of uncoated and coated cutting tools is shown in Fig. 12. The abrasive wear on the flank surface of the TiAlSiN coated tool was very smooth, with no evidence of micro-grooves that may form during material erosion on the flank surface of the tool owing to rubbing of the tool with the workpiece. The uncoated ceramic tool, DLC, and WC/C coated tools, on the other hand, showed flank wear with micro-groove development. The WC/C coated tool, on the other hand, had a smoother abrasive wear than the DLC coated tool and the uncoated cutting tool. The cutting tools with low friction coatings and TiAlSiN coating showed no signs of significant wear till 200 m/min whereas at 250 m/min there was significant coating delamination (see Fig. 12) exposing the ceramic substrate leading to formation of micro-grooves for both DLC and WC/C coated tools. This, has led to the increase in machining forces for the cutting tools coated with DLC and WC/C coatings at 250 m/min cutting speed. On the contrary, the TiAlSiN coating due to its higher hardness and coating/substrate adhesion strength showed minimal wear even at 250 m/min cutting speed and thus, there is further reduction of machining forces with the increase of cutting speed.

4. Conclusions

The performance of TiAlSiN, DLC, and WC/C coated Al_2O_3/TiC cutting tools during hard turning of AISI 52100 steel was investigated in this study. The following are some of the conclusions that can be derived from the findings:

1. The deposition of coatings on the surface of cutting tools resulted in reduction of machining forces. The low friction coatings although softer when compared to the Al_2O_3/TiC substrate, resulted in significant reduction in machining forces when compared to the uncoated cutting tool.
2. The low-friction coatings resulted in considerable reduction in friction whereas the TiAlSIN coating exhibited the highest friction values for cutting speeds up to 200. The coefficient of friction for TiAlSiN coated tool drops to a value similar to that of cutting tools coated with low-friction coatings at 250 m/min. Also, when compared to the low-friction DLC and WC/C coatings, the TiAlSiN coating exhibited continuous reduction of machining forces and friction with the increase of cutting speed showing the superiority of the coating at adverse machining conditions. The superior performance of the TiAlSiN coating can be attributed to its higher hardness, coating/substrate adhesion strength, thermal stability and oxidation resistance as compared to the other films.
3. The reduction of friction and machining forces leading to lower strain along the shear plane accounted to lower deformation of the chips and thus, lower friction accounted to lower values of C_w, C_T, Th_{maj} and Th_{min}. On the contrary, the teeth bend angle showed inverse relation to the coefficient of friction due to reduction of localized stresses at the tip of the serrated teeth.
4. The TiAlSiN coated tool had a smoother wear pattern and showed less wear on the rake surface. Furthermore, at 250 m/min cutting speed, the DLC and WC/C coatings resulted in smoother abrasion than the uncoated cutting tool, but they were not successful in preventing micro-groove formation on the flank surface during the machining process.

The TiAlSiN coating, with its nanocomposite structure, high hardness, and higher coating/substrate adhesion strength, outperformed DLC and WC/C coatings at the greatest cutting speed, according to the results of this study. However, due to their self-lubricating qualities, the DLC and WC/C coatings, despite being softer, accounted for a large reduction in machining forces.

Declaration of Competing Interest

The authors declare that they have no known competing financial interests or personal relationships that could have appeared to influence the work reported in this paper.

Acknowledgement

This work is sponsored by FEDER National funds FCT under the projects: SMARTLUB “Smart self-lubricant coatings with controlled release of the lubricious agent for high temperature applications.” (ref. “POCI-01-0145-FEDER-031807”), MCTool21 “Manufacturing of cutting tools for the 21st century: from nano-scale material design to numerical process simulation” (ref.: “POCI-01-0247-FEDER-045940”) and CEMMPRE ref. “UIDB/00285/2020”.

REFERENCES

[1] Tönshoff HK, Arendt C, ben Amor R. Cutting of hardened steel. CIRP Ann - Manuf Technol 2000;49:547–66. https://doi.org/10.1016/S0007-8506(07)63455-6.

[2] Umbrello D, Hua J, Shivpuri R. Hardness-based flow stress and fracture models for numerical simulation of hard machining AISI 52100 bearing steel. Mater Sci Eng 2004;374:90–100. https://doi.org/10.1016/j.msea.2004.01.012.

[3] Umbrello D, Rizzuti S, Outeiro JC, Shivpuri R, Saoubi RM, Ab T, et al. Hardness-based flow stress for numerical simulation of hard machining AISI H13 tool steel, vol. 9; 2007. p. 64–73. https://doi.org/10.1016/j.jmatprotec.2007.08.018.

[4] Grzesik W, Wanat T. Comparative assessment of surface roughness produced by hard machining with mixed ceramic tools including 2D and 3D analysis. J Mater Process Technol 2005;169:364–71. https://doi.org/10.1016/j.jmatprotec.2005.04.080.
[5] Chinchanikar S, Choudhury SK. Hard turning using HiPIMS-coated carbide tools: wear behavior under dry and minimum quantity lubrication (MQL), Measurement. J Int Measure Confederation 2014;55:536–48. https://doi.org/10.1016/j.measurement.2014.06.002.
[6] Grzesik W, Rech J, Wanat T. Surface finish on hardened bearing steel parts produced by superhard and abrasive tools. Int J Mach Tool Manufact 2007;47:255–62. https://doi.org/10.1016/j.ijmachtools.2006.03.018.
[7] Hua J, Umbrello D, Shivpuri R. Investigation of cutting conditions and cutting edge preparations for enhanced compressive subsurface residual stress in the hard turning of bearing steel. J Mater Process Technol 2006;171:180–7. https://doi.org/10.1016/j.jmatprotec.2005.06.087.
[8] Kumar ChS, Patel SK. Performance analysis and comparative assessment of nano-composite TiAlSiN/TiSiN/TiAlN coating in hard turning of AISI 52100 steel. Surf Coating Technol 2018;335:265–79. https://doi.org/10.1016/j.surfcoat.2017.12.048.
[9] Sales WF, Costa LA, Santos SC, Diniz AE, Bonney J, Ezugwu EO. Performance of coated, cemented carbide, mixed-ceramic and PCBN-H tools when turning W320 steel. Int J Adv Manuf Technol 2009;41:660–9. https://doi.org/10.1007/s00170-008-1523-4.
[10] Sobiyi K, Sigalas I, Akdogan G, Turan Y. Performance of mixed ceramics and CBN tools during hard turning of martensitic stainless steel. Int J Adv Manuf Technol 2015;77:861–71. https://doi.org/10.1007/s00170-014-6506-z.
[11] Kumar CS, Patel SK. Investigations on the effect of thickness and structure of AlCr and AlTi based nitride coatings during hard machining process. J Manuf Process 2018;31:336–47. https://doi.org/10.1016/j.jmapro.2017.11.031.
[12] Sateesh Kumar C, Kumar Patel S. Hard machining performance of PVD AlCrN coated Al2O3/TiCN ceramic inserts as a function of thin film thickness. Ceram Int 2017;43:13314–29. https://doi.org/10.1016/j.ceramint.2017.07.030.
[13] An Q, Wang C, Xu J, Liu P, Chen M. Experimental investigation on hard milling of high strength steel using PVD-AlTiN coated cemented carbide tool. Int J Refract Metals Hard Mater 2014;43:94–101. https://doi.org/10.1016/j.ijrmhm.2013.11.007.
[14] Kumar CS, Patel SK. Effect of duplex nanostructured TiAlSiN/TiSiN/TiAlN-TiAlN and TiAlN-TiAlSiN/TiSiN/TiAlN coatings on the hard turning performance of Al 2 O 3 -TiCN ceramic cutting tools. Wear 2019;418–419:226–40. https://doi.org/10.1016/j.wear.2018.11.013.
[15] Das SR, Dhupal D, Kumar A. Experimental investigation into machinability of hardened AISI 4140 steel using TiN coated ceramic tool, Measurement. J Int Measure Confederation 2015;62:108–26. https://doi.org/10.1016/j.measurement.2014.11.008.
[16] El Hakim MA, Abad MD, Abdelhameed MM, Shalaby MA, Veldhuis SC. Wear behavior of some cutting tool materials in hard turning of HSS. Tribol Int 2011;44:1174–81. https://doi.org/10.1016/j.triboint.2011.05.018.
[17] Brzezinka T, Rao J, Paiva J, Kohlscheen J, Fox-Rabinovich G, Veldhuis S, et al. DLC and DLC-WS2 coatings for machining of aluminium alloys. Coatings 2019;9:192. https://doi.org/10.3390/coatings9030192.
[18] Viana R, Machado AR. Influence of adhesion between coating and substrate on the performance of coated HSS twist drills. J Braz Soc Mech Sci Eng 2009;31:327–32. https://doi.org/10.1590/S1678-58782009000400007.
[19] Ucun I, Aslantas K, Bedir F. The performance of DLC-coated and uncoated ultra-fine carbide tools in micromilling of Inconel 718. Precis Eng 2015;41:135–44. https://doi.org/10.1016/j.precisioneng.2015.01.002.
[20] Derflinger V, Brändle H, Zimmermann H. New hard/lubricant coating for dry machining. Surf Coating Technol 1999;113:286–92. https://doi.org/10.1016/S0257-8972(99)00004-3.
[21] Sateesh Kumar C, Majumder H, Khan A, Patel SK. Applicability of DLC and WC/C low friction coatings on Al2O3/TiCN mixed ceramic cutting tools for dry machining of hardened 52100 steel. Ceram Int 2020;46:11889–97. https://doi.org/10.1016/j.ceramint.2020.01.225.
[22] Das P, Anwar S, Bajpai S, Anwar S. Structural and mechanical evolution of TiAlSiN nanocomposite coating under influence of Si3N4 power. Surf Coating Technol 2016;307:676–82. https://doi.org/10.1016/j.surfcoat.2016.09.065.
[23] Tallant DR, Parmeter JE, Siegal MP, Simpson RL. The thermal stability of diamond-like carbon. Diam Relat Mater 1995;4:191–9. https://doi.org/10.1016/0925-9635(94)00243-6.
[24] Dobrzański LA, Pakuła D, Křiž A, Soković M, Kopač J. Tribological properties of the PVD and CVD coatings deposited onto the nitride tool ceramics. J Mater Process Technol 2006;175:179–85. https://doi.org/10.1016/j.jmatprotec.2005.04.032.
[25] Barshilia HC, Ghosh M, Shashidhara, Ramakrishna R, Rajam KS. Deposition and characterization of TiAlSiN nanocomposite coatings prepared by reactive pulsed direct current unbalanced magnetron sputtering. Appl Surf Sci 2010;256:6420–6. https://doi.org/10.1016/j.apsusc.2010.04.028.
[26] Du J, Hao T, Zhang X, Su G, Zhang P, Sun Y, et al. Finite element investigation of cutting performance of Cr/W-DLC/DLC composite coated cutting tool. Int J Adv Manuf Technol 2022;118:2177–92. https://doi.org/10.1007/s00170-021-08093-0.
[27] Yin Z, Huang C, Zou B, Liu H, Zhu H, Wang J. High temperature mechanical properties of Al2O3/TiC micro-nano-composite ceramic tool materials. Ceram Int 2013;39:8877–83. https://doi.org/10.1016/j.ceramint.2013.04.081.
[28] Fukuhara M, Fukazawa K, Fukawa A. Physical properties and cutting performance of silicon nitride ceramic. Wear 1985;102:195–210. https://doi.org/10.1016/0043-1648(85)90218-2.
[29] Kržan B, Novotny-Farkas F, Vižintin J. Tribological behavior of tungsten-doped DLC coating under oil lubrication. Tribol Int 2009;42:229–35. https://doi.org/10.1016/j.triboint.2008.06.011.
[30] Bernardes CF, Fukumasu NK, Machado GAA, Machado IF. Tribological behavior of DLC and WDLC carbon based coatings during reciprocating wear tests. SAE Technical Papers; 2017. https://doi.org/10.4271/2017-36-0254. 2017-Novem.
[31] Fukui H, Okida J, Omori N, Moriguchi H, Tsuda K. Cutting performance of DLC coated tools in dry machining aluminum alloys. Surf Coating Technol 2004;187:70–6. https://doi.org/10.1016/j.surfcoat.2004.01.014.
[32] Thakur A, Mohanty A, Gangopadhyay S, Maity KP. Tool wear and chip characteristics during dry turning of inconel 825. Procedia Materials Science 2014;5:2169–77. https://doi.org/10.1016/j.mspro.2014.07.422.
[33] Jiang F, Yan L, Rong Y. Orthogonal cutting of hardened AISI D2 steel with TiAlN-coated inserts - simulations and experiments. Int J Adv Manuf Technol 2013;64:1555–63. https://doi.org/10.1007/s00170-012-4122-3.

[34] Thakur A, Gangopadhyay S, Mohanty A. Investigation on some machinability aspects of inconel 825 during dry turning. Mater Manuf Process 2015;30:1026–34. https://doi.org/10.1080/10426914.2014.984216.

[35] Mohanty A, Gangopadhyay S, Thakur A. On applicability of multilayer coated tool in dry machining of aerospace grade stainless steel. Mater Manuf Process 2016;31:869–79. https://doi.org/10.1080/10426914.2015.1070413.